Dalton Transactions

PAPER

View Article Online
View Journal | View Issue

Cite this: *Dalton Trans.*, 2015, **44**, 16313

Dinuclear copper(I) complexes with N-heterocyclic thione and selone ligands: synthesis, characterization, and electrochemical studies†

Martin M. Kimani,[a] David Watts,[a] Leigh A. Graham,[b] Daniel Rabinovich,[b] Glenn P. A. Yap[c] and Julia L. Brumaghim*[a]

Received 11th June 2015,
Accepted 18th August 2015

DOI: 10.1039/c5dt02232k

www.rsc.org/dalton

The synthesis, characterization, and structures of a series of homoleptic and heteroleptic copper(I) complexes supported by N-heterocyclic chalcogenone ligands is reported herein. The quasi-reversible Cu(II/I) reduction potentials of these copper complexes with monodentate (dmit or dmise) and/or bidentate (Bmm^{Me}, $Bsem^{Me}$, Bme^{Me}, $Bsee^{Me}$) chalcogenone ligands are highly dependent upon the nature and number of the donor groups and can be tuned over a 470 mV range (−369 to 102 mV). Copper–selone complexes have more negative Cu(II/I) reduction potentials relative to their thione analogs by an average of 137 mV, and increasing the number of methylene units linking the heterocyclic rings in the bidentate ligands results in more negative reduction potentials for their copper complexes. This ability to tune the copper reduction potentials over a wide range has potential applications in synthetic and industrial catalysis as well as the understanding of important biological processes such as electron transfer in blue copper proteins and respiration.

Introduction

The chemistry of monodentate and bidentate sulfur and selenium Lewis donor ligands towards soft and borderline metals has recently received much attention due to their potential applications in catalysis,[1,2] the preparation of radiopharmaceuticals,[3] and in supramolecular, bioinorganic, organometallic, and coordination chemistry.[4,5] Thus, great strides have been made in understanding the coordination chemistry of bis(mercaptoimidazolyl)borate (Bm^R) and bis(mercaptoimidazolyl)-methane (Bmm^R) ligands, first pioneered by Parkin[6,7] and Williams,[8] respectively. In contrast, the reactivity of the corresponding selenium analogs, the bis(selenoimidazolyl)borates (Bse^R),[9,10] bis(selenoimidazolyl)methanes ($Bsem^R$),[1,11] and related derivatives,[5] remains markedly underdeveloped.

We are interested in the coordination chemistry of the aforementioned bidentate neutral ligands as well as that of the closely related bis(mercaptoimidazolyl)ethanes (Bme^R) and bis(selenoimidazolyl)ethanes ($Bsee^R$) with copper(I) to understand the fundamentals of the copper–sulfur and copper–selenium interactions and their effect on Cu(I)/Cu(II) redox potentials. The high propensity for sulfur- and selenium-containing ligands to bridge metal centers also results in diverse coordination frameworks[12] and these groups are also potential synthons for the formation of heterocyclic carbenes *via* potassium metal reduction.[13] There is also increased interest in copper chalcogenolates as single-source precursors in the synthesis of semiconductor materials *via* metal organic chemical vapor deposition.[14]

Although coordination complexes of the Bmm^{Me} ligand with rhenium(I),[3] iron(II),[15] cobalt(II),[11] rhodium(I),[1,16] iridium(I),[17] nickel(II),[11] silver(I),[18,19] gold(I/III),[19] zinc(II),[20] tin(II),[21] lead(II)[22,23] and antimony(III)[8] have been isolated, it is rather surprising that only one report of copper(I) derivatives has been published,[19] particularly given the reported affinity of copper for sulfur- and selenium-containing ligands.[24]

In this work, we report the synthesis and crystal structures of a series of dinuclear, three- and four-coordinate copper(I) complexes with the aim of understanding the effect of the methylene linkers and chalcogenone donor groups on the redox potentials of the Cu(I)/Cu(II) couple. These reduction potentials are highly dependent upon S/Se ligand coordination and can be tuned in a wide potential range using a variety of monodentate and bidentate thione and selone ligands. Such

[a]*Department of Chemistry, Clemson University, Clemson, SC 29634-0973, USA. E-mail: brumagh@clemson.edu*
[b]*Department of Chemistry, The University of North Carolina at Charlotte, 9201 University City Boulevard, Charlotte, NC 28223, USA*
[c]*Department of Chemistry and Biochemistry, The University of Delaware, Newark, DE 19716, USA*

†Electronic supplementary information (ESI) available: Crystal packing diagram of **10** (Fig. S1), cyclic voltammograms of complexes **1–10** (Fig. S2). CCDC 1405705–1405711. For ESI and crystallographic data in CIF or other electronic format see DOI: 10.1039/c5dt02232k

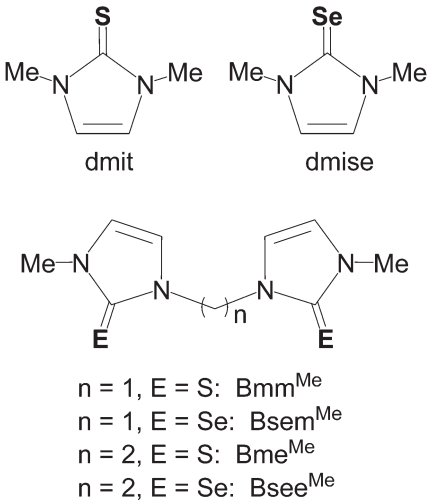

Fig. 1 Chalcogenone ligands used in this study.

redox tuning has practical applications ranging from understanding biological processes such as electron transfer in blue copper proteins and respiration,[25] to industrial and synthetic applications in catalysis.[2,26] Homoleptic and heteroleptic copper(I) complexes bearing monodentate (dmit or dmise) or bidentate (Bmm^{Me}, $Bsem^{Me}$, Bme^{Me}, $Bsee^{Me}$) chalcogenone ligands (Fig. 1) have been synthesized and characterized using elemental analysis, infrared (IR) and multinuclear (^1H, ^{13}C, ^{19}F, ^{77}Se) NMR spectroscopies, single-crystal X-ray diffraction, electrospray ionization mass spectrometry, and cyclic voltammetry.

Results and discussion

Synthesis of dinuclear copper(I) thione and selone complexes

Homoleptic dinuclear copper complexes were synthesized *via* the reaction of $[Cu(NCMe)_4]BF_4$ with the appropriate amount of *N*,*N*′-dimethylimidazole thione (dmit) or *N*,*N*′-dimethylimidazole selone (dmise) in acetonitrile (eqn (1)) or bis(mercaptoimidazolyl)methane (Bmm^{Me}), bis(selenoimidazolyl)-methane ($Bsem^{Me}$), bis(mercaptoimidazolyl)ethane (Bme^{Me}), and bis(selenoimidazolyl)ethane ($Bsee^{Me}$) in a mixed-solvent system of acetonitrile and dichloromethane (eqn (2)).

$$[Cu(NCMe)_4]BF_4 + 2.5\ L \xrightarrow{MeCN} \underset{\substack{L=dmit(\mathbf{1})\\L=dmise(\mathbf{2})}}{[L_2Cu(\mu\text{-}L)CuL_2](BF_4)_2} \quad (1)$$

$$[Cu(NCMe)_4]BF_4 + 1.5\ L \xrightarrow{MeCN/CH_2Cl_2} \underset{\substack{L=Bmm^{Me}\ (\mathbf{3})\\L=Bsem^{Me}\ (\mathbf{4})\\L=Bme^{Me}\ (\mathbf{5})\\L=Bsee^{Me}\ (\mathbf{6})}}{[LCu(\mu\text{-}L)CuL](BF_4)_2} \quad (2)$$

$$[Cu(NCMe)_4]BF_4 \xrightarrow[(2)\ L',\ CH_2Cl_2]{(1)\ L,\ MeCN} \underset{\substack{L=dmit,\ L'=Bsem^{Me}\ (\mathbf{7})\\L=dmise,\ L'=Bmm^{Me}\ (\mathbf{8})\\L=dmise,\ L'=Bsem^{Me}\ (\mathbf{9})}}{[LCu(\mu\text{-}L')_2CuL](BF_4)_2} \quad (3)$$

$$[Cu(NCMe)_4]BF_4 \xrightarrow[(2)\ Bmm^{Me},\ CH_2Cl_2]{(1)\ dmit,\ MeCN} \underset{(\mathbf{10})}{[(Bmm^{Me})Cu(\mu\text{-}dmit)]_n(BF_4)_n} \quad (4)$$

In turn, heteroleptic dinuclear complexes of copper(I) were synthesized *via* a convenient two-step, one-pot synthesis by treating equimolar amounts of $[Cu(NCMe)_4]BF_4$ and dmit or dmise in acetonitrile, followed by cannula addition of Bmm^{Me} or $Bsem^{Me}$ in dichloromethane (eqn (3)). Similarly, treating equimolar amounts of $[Cu(NCMe)_4]BF_4$ and dmit in acetonitrile followed by addition of one molar equivalent of Bmm^{Me} in dichloromethane afforded a polynuclear copper(I) complex (eqn (4)).

Structural analyses of dinuclear copper complexes

The molecular structures of several complexes have been obtained using X-ray crystallography. More specifically, single crystals suitable for X-ray diffraction studies were obtained for $[(dmise)_2Cu(\mu\text{-}dmise)Cu(dmise)_2](BF_4)_2\cdot CH_3CN$ (**2**), $[(Bmm^{Me})Cu(\mu\text{-}Bmm^{Me})Cu(Bmm^{Me})](BF_4)_2$ (**3**), $[(Bsem^{Me})Cu(\mu\text{-}Bsem^{Me})Cu(Bsem^{Me})](BF_4)_2$ (**4**), $[(Bme^{Me})Cu(\mu\text{-}Bme^{Me})Cu(Bme^{Me})](BF_4)_2$ (**5**), $[(dmit)Cu(\mu\text{-}Bsem^{Me})_2Cu(dmit)](BF_4)_2$ (**7**), $[(dmise)Cu(\mu\text{-}Bsem^{Me})_2Cu(dmise)](BF_4)_2$ (**9**), and $[(Bmm^{Me})Cu(\mu\text{-}dmit)]_n(BF_4)_n$ (**10**).

The X-ray crystal structure of $[(dmise)_2Cu(\mu\text{-}dmise)Cu(dmise)_2](BF_4)_2\cdot CH_3CN$ (**2**), is shown in Fig. 2, and selected bond lengths (Å) and angles (°) are given in Table 1. The structural unit of $[(dmise)_2Cu(\mu\text{-}dmise)Cu(dmise)_2](BF_4)_2$ is made up of two copper(I) centers, with the Se atom of the dimethylimidazole selone (dmise) ligands bridging the two copper atoms, forming a bent CuSeCu core. Each copper atom is further bonded to two dmise ligands and thus each copper adopts a distorted trigonal planar geometry. The average of the

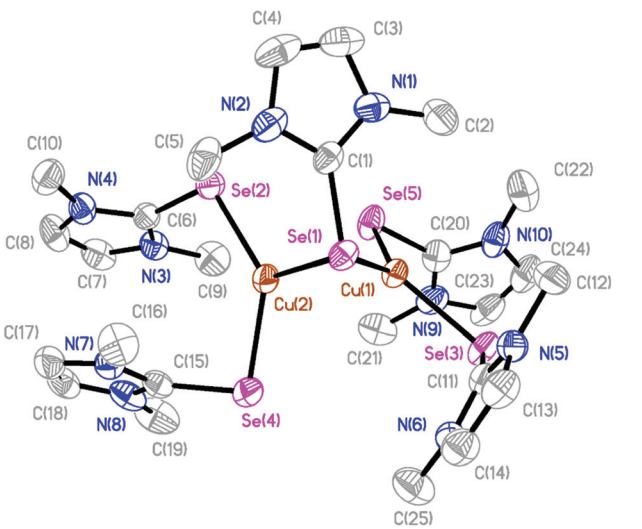

Fig. 2 The crystal structure diagram of the cation in $[(dmise)_2Cu(\mu\text{-}dmise)Cu(dmise)_2](BF_4)_2\cdot CH_3CN$ (**2**) showing 50% probability ellipsoids. Hydrogen atoms, counterions, and the solvent molecules are omitted for clarity.

Table 1 Selected bond lengths (Å) and angles (°) for **2**

Cu(1)–Se(1)	2.3986(9)	Se(5)–Cu(1)–Se(3)	118.37(4)
Cu(2)–Se(1)	2.4382(10)	Se(5)–Cu(1)–Se(1)	128.11(4)
Cu(1)–Se(3)	2.3460(10)	Se(3)–Cu(1)–Se(1)	113.34(3)
Cu(1)–Se(5)	2.3377(9)	Se(2)–Cu(1)–Se(4)	133.26(4)
Cu(2)–Se(2)	2.3458(11)	Se(2)–Cu(1)–Se(1)	111.91(4)
Cu(2)–Se(4)	2.3592(12)	Se(4)–Cu(1)–Se(1)	112.68(4)
Cu(1)–Cu(2)	2.6326(11)		

four Cu–Se distances involving terminal dmise ligands (2.35 Å) is shorter than those involving the bridging dmise ligand (2.42 Å) but is slightly longer than those in the monomeric copper selone complexes (~2.30 Å) reported by Kimani *et al.*[27] In a similar vein, these values are comparable to those observed in the three-coordinate copper selone complexes $Cu(dmise)_2X$, (X = Cl, Br, I)[28] and the diphosphine selenide derivative $[Cu_3I_3\{Ph_2P(Se)\text{–}(CH_2)_3\text{–}P(Se)Ph_2\}_2]_n$.[29]

The molecular structures of the isostructural complexes $[(Bmm^{Me})Cu(\mu\text{-}Bmm^{Me})Cu(Bmm^{Me})](BF_4)_2$ (**3**) and $[(Bsem^{Me})Cu(\mu\text{-}Bsem^{Me})Cu(Bsem^{Me})](BF_4)_2$ (**4**) are shown in Fig. 3 and 4, with selected bond lengths and angles given in Tables 2 and 3, respectively. The dinuclear complexes feature two terminal and one bridging bis(chalcogenone) ligands, forming "butterfly" shape $[Cu_2E_2]$ cores (E = S, Se). Each copper(I) ion adopts a distorted tetrahedral geometry, with angles ranging from 96.45 to 123.86° for **3** and from 100.50 to 123.36° for **4**. The Cu···Cu distances (2.96 and 2.97 Å for **3** and **4**, respectively), significantly longer than twice the covalent radius of copper(I) (2.34 Å), precludes the existence of a copper–copper bonding interaction in these complexes. As expected, the terminal Cu–S and Cu–Se bond distances in **3** and **4** (averages 2.29 and 2.42 Å, respectively) and shorter than those involving the corresponding values involving bridging ligands (averages 2.44 and 2.52 Å, respectively).

The centrosymmetric copper complex $[(Bme^{Me})Cu(\mu\text{-}Bme^{Me})Cu(Bme^{Me})](BF_4)_2$ (**5**) (Fig. 5) exhibits two copper(I)

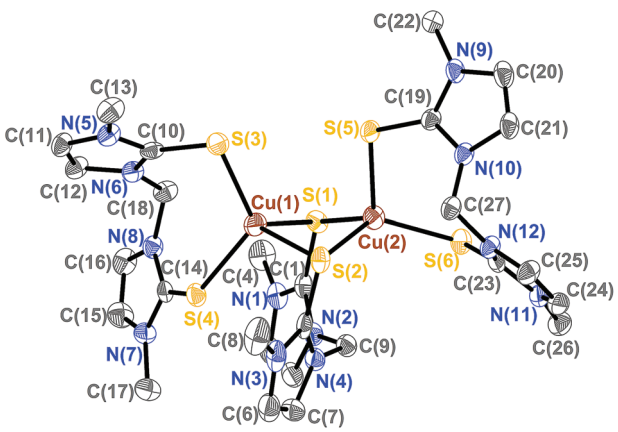

Fig. 3 The crystal structure diagram of the cation in $[(Bmm^{Me})Cu(\mu\text{-}Bmm^{Me})Cu(Bmm^{Me})](BF_4)_2$ (**3**) showing 50% probability ellipsoids. Hydrogen atoms and counterions are omitted for clarity.

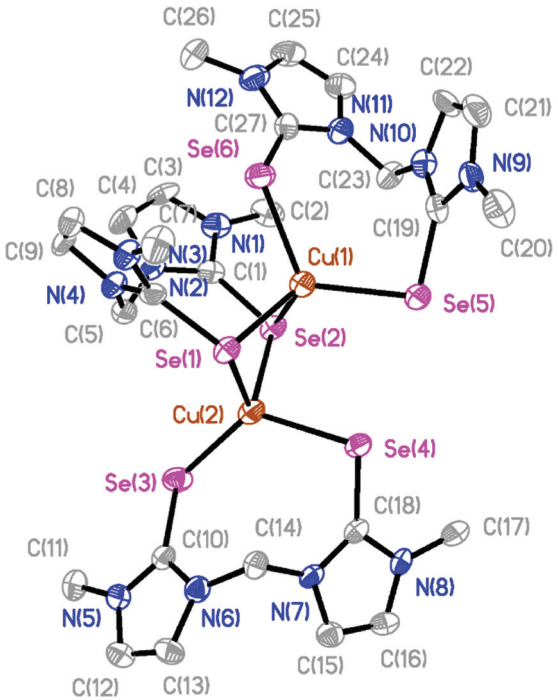

Fig. 4 The crystal structure diagram of the cation in $[(Bsem^{Me})Cu(\mu\text{-}Bsem^{Me})Cu(Bsem^{Me})](BF_4)_2$ (**4**) showing 50% probability ellipsoids. Hydrogen atoms, counterions, and solvent molecules are omitted for clarity.

Table 2 Selected bond distances (Å) and angles (°) for **3**

Cu(1)–S(1)	2.6675(17)	S(1)–Cu(1)–S(2)	96.45(4)
Cu(1)–S(2)	2.3338(15)	S(1)–Cu(1)–S(3)	113.78(6)
Cu(1)–S(3)	2.2710(16)	S(1)–Cu(1)–S(4)	105.57(5)
Cu(1)–S(4)	2.3067(15)	S(2)–Cu(1)–S(3)	118.32(5)
Cu(2)–S(1)	2.3006(15)	S(2)–Cu(1)–S(4)	103.97(6)
Cu(2)–S(2)	2.4706(16)	S(3)–Cu(1)–S(4)	116.26(5)
Cu(2)–S(5)	2.2964(16)	S(1)–Cu(2)–S(2)	103.03(5)
Cu(2)–S(6)	2.3033(14)	S(1)–Cu(2)–S(5)	107.51(5)
Cu(1)–Cu(2)	2.9741(13)	S(1)–Cu(2)–S(6)	112.87(5)
		S(2)–Cu(2)–S(5)	96.51(5)
		S(2)–Cu(2)–S(6)	123.86(5)
		S(5)–Cu(2)–S(6)	111.07(5)

Table 3 Selected bond distances (Å) and angles (°) for **4**

Cu(1)–Se(1)	2.5128(12)	Se(1)–Cu(1)–Se(2)	100.50(4)
Cu(1)–Se(2)	2.5617(13)	Se(1)–Cu(1)–Se(5)	115.76(4)
Cu(1)–Se(5)	2.4221(11)	Se(1)–Cu(1)–Se(6)	100.21(4)
Cu(1)–Se(6)	2.4315(12)	Se(2)–Cu(1)–Se(5)	110.93(4)
Cu(2)–Se(1)	2.5073(12)	Se(2)–Cu(1)–Se(6)	113.12(5)
Cu(2)–Se(2)	2.4981(12)	Se(5)–Cu(1)–Se(6)	115.10(5)
Cu(2)–Se(3)	2.4091(15)	Se(1)–Cu(2)–Se(2)	102.43(4)
Cu(2)–Se(4)	2.4267(11)	Se(1)–Cu(2)–Se(3)	122.52(4)
Cu(1)–Cu(2)	2.9616(18)	Se(1)–Cu(2)–Se(4)	95.13(4)
		Se(2)–Cu(2)–Se(3)	107.50(4)
		Se(2)–Cu(2)–Se(4)	102.71(4)
		Se(3)–Cu(2)–Se(4)	123.36(4)

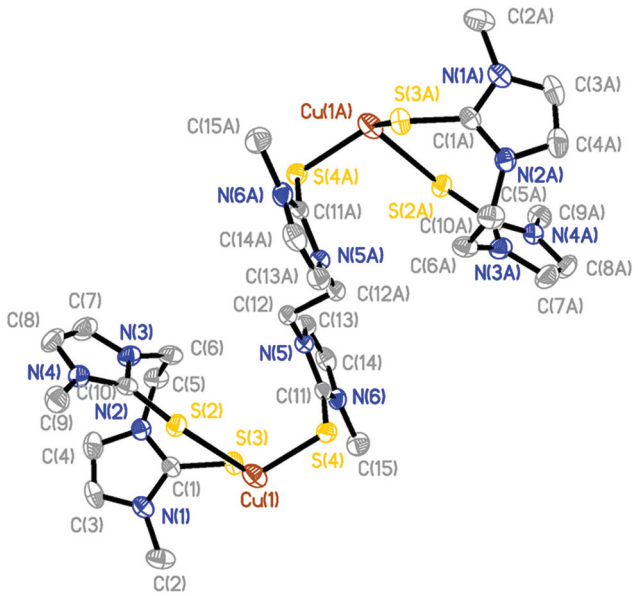

Fig. 5 Crystal structure diagram of the cation in $[(Bme^{Me})Cu(\mu\text{-}Bme^{Me})\text{-}Cu(Bme^{Me})](BF_4)_2$ (**5**) displaying 50% probability density ellipsoids. Hydrogen atoms and counterions are omitted for clarity.

centers, each arranged in a distorted trigonal planar geometry arising from the coordination of a terminal bidentate Bme^{Me} ligand and one of the thione moieties from a bridging bis-(monodentate) Bme^{Me} ligand. As summarized in Table 4, the sum of angles around each copper center is 354.91° and the average C–S bond distance is 2.29 Å.

The molecular structures of $[(dmit)Cu(\mu\text{-}Bsem^{Me})_2Cu(dmit)](BF_4)_2$ (**7**) and $[(dmise)Cu(\mu\text{-}Bsem^{Me})_2Cu(dmise)](BF_4)_2$ (**9**) are shown in Fig. 6, with selected bond length and angles for the isostructural complexes given in Table 5. The two dinuclear complexes are centrosymmetric and exhibit rhombic Cu_2Se_2 cores, with all the bis(selone) ligands exhibiting the unusual bridging monodentate:bidentate ($\mu\text{–}\kappa^1\text{:}\kappa^2$) coordination mode. Each copper center is coordinated to a terminal dmit or dmise ligand and three selone moieties from $Bsem^{Me}$ ligands (one terminal and two bridging), with an overall distorted tetrahedral geometry in each case. The angles surrounding the copper centers in the two complexes are very similar, ranging from 95.38 to 118.61° for **7** and from 94.97 to 118.58° for **9**. The Cu···Cu distances (2.73 and 2.74 Å for **7** and **9**, respectively) are slightly shorter than the sum of the van der Waals radii of copper, suggesting the presence of weak Cu–Cu interactions.

Table 4 Selected bond lengths (Å) and angles (°) for **5**

Cu(1)–S(4)	2.2871(16)
Cu(1)–S(3)	2.3030(16)
Cu(1)–S(2)	2.2900(14)
S(4)–Cu(1)–S(2)	122.49(5)
S(4)–Cu(1)–S(3)	114.70(6)
S(3)–Cu(1)–S(2)	117.72(5)

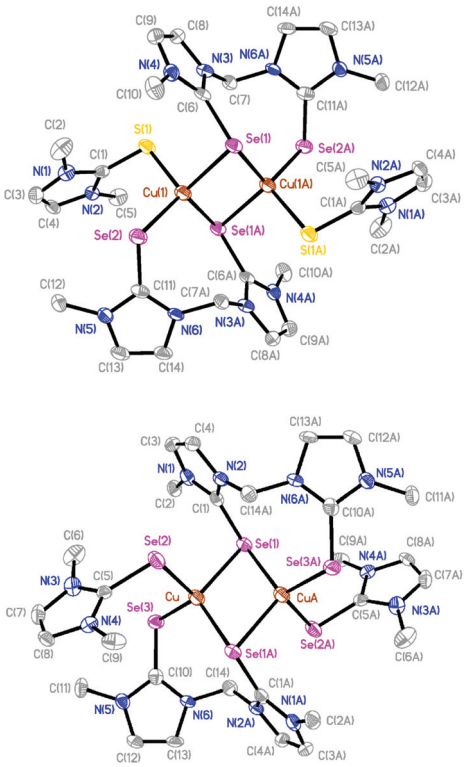

Fig. 6 Crystal structure diagrams of the cations in $[(dmit)Cu(\mu\text{-}Bsem^{Me})_2\text{-}Cu(dmit)](BF_4)_2$ (**7**, top) and $[(dmise)Cu(\mu\text{-}Bsem^{Me})_2Cu(dmise)](BF_4)_2$ (**9**, bottom) showing 50% probability ellipsoids. Hydrogen atoms and counterions are omitted for clarity.

Table 5 Selected bond distances (Å) and angles (°) for **7** and **9**

7		**9**	
Cu(1)–S(1)	2.3455(16)	Cu–Se(1)	2.5349(12)
Cu(1)–Se(2)	2.4222(12)	Cu–Se(A1)	2.4950(13)
Cu(1)–Se(1A)	2.5013(11)	Cu–Se(2)	2.4583(13)
Cu(1)–Se(1)	2.5328(11)	Cu–Se(3)	2.4238(14)
Se(1)–Cu(1A)	2.5013(11)	Cu(A)–Se(1)	2.4950(13)
Cu(1)–Cu(1A)	2.7297(19)	Cu–Cu(A)	2.739(2)
S(1)–Cu(1)–Se(2)	116.36(6)	Se(1)–Cu–Se(2)	105.02(5)
S(1)–Cu(1)–Se(1A)	95.38(5)	Se(1)–Cu–Se(3)	107.35(5)
Se(2)–Cu(1)–Se(1A)	118.61(4)	Se(1)–Cu–Se(A1)	114.02(5)
S(1)–Cu(1)–Se(1)	105.58(5)	Se(2)–Cu–Se(3)	115.95(5)
Se(2)–Cu(1)–Se(1)	105.96(4)	Se(2)–Cu–Se(A1)	94.97(5)
Se(1A)–Cu(1)–Se(1)	114.33(4)	Se(3)–Cu–Se(A1)	118.58(4)

The average lengths of the bridging Cu–Se bonds derived from $Bsem^{Me}$ ligands (2.52 and 2.51 Å for **7** and **9**, respectively) are longer than the average terminal Cu–Se bond lengths associated with the same ligands (2.42 Å for both complexes).

The X-ray structure of $[(Bmm^{Me})Cu(\mu\text{-dmit})]_n(BF_4)_n$ (**10**), unlike all the ones described above, reveals the formation of a coordination polymer in which an infinite chain of four-coordinate copper(I) centers are bound to two terminal sulfur atoms from a bidentate Bmm^{Me} ligand and two sulfur atoms from bridging dmit ligands (Fig. 7 and ESI, Fig. S1†). The geo-

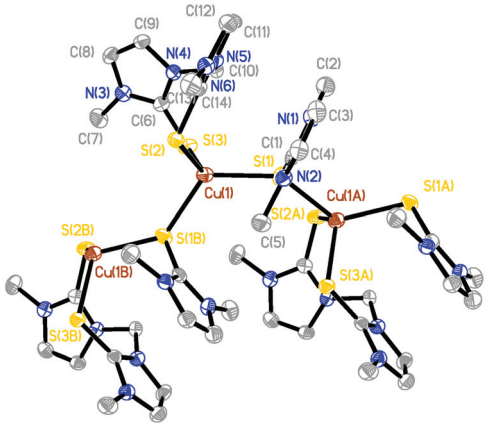

Fig. 7 Crystal structure diagram of the cationic portion of $[(Bmm^{Me})Cu(\mu\text{-dmit})]_n(BF_4)_n$ (**10**) showing three repeating units of the coordination polymer and 50% probability ellipsoids. Hydrogen atoms and counterions are omitted for clarity.

metry around Cu(1) is best described as distorted tetrahedral, with S–Cu–S angles ranging from 95.06° to 123.18°, and average Cu–S bond lengths of 2.36 Å (Table 6).

Although the number of reported N-heterocyclic thione and selone complexes of copper(I) is limited, further comparison of the metrical parameters observed in the structures described above can be made. The tetrahedrally coordinated dinuclear copper selone complexes **4**, **7**, and **9** have average terminal Cu–Se bond lengths of 2.43 Å, longer than the average terminal Cu–Se bond distances of 2.30 Å for $[(Tpm^R)Cu(dmise)][BF_4]$ (R = H, Me, iPr), 2.33 Å for Tp*Cu(dmise),[27] and an average of 2.41 Å for $[Cu(C_{11}H_{14}Se_2)_2][BF_4]$,[30] but shorter than the 2.49 Å in $[Cu(1,10\text{-phen})_2(C_5H_{10}N_2Se)][2ClO_4]$.[31] The Se–C bonds in **2**, in the range of 1.85–1.88 Å, are slightly lengthened relative to those in uncoordinated dmise (1.89 Å).[32]

In a similar vein, the copper thione complexes **3**, **5**, **7** and **10** have an average terminal Cu–S bond distance of 2.34 Å, longer than the corresponding terminal bond distances observed in most previously reported copper thione and thiolate complexes, including $[(Tpm^R)Cu(dmit)]BF_4$ (2.20 Å; R = H, Me), Tp*Cu(dmit),[27] $[Cu(diditme)_2Cl]$ (2.23 Å),[33] $Cu_3(Bm^{Me})_3$ (~2.28 Å), $(Bm^{Me})Cu(PPh_3)$ (2.28 Å),[34] but somewhat shorter than those in $[Cu(PPh_3)_2(bzimH_2)Cl]$ (2.38 Å),[35] $[CuCl(1\kappa S\text{-}imzSH)(PPh_3)_2]$ (2.36 Å),[36] and significantly shorter than in $[Cu(HB(3,5\text{-}iPrPz)_3(SMeIm)]$ (2.45 Å).[37] The S–C bond lengths in complexes **6**, **8**, and **10** (in the range 1.694–1.704 Å), are slightly lengthened relative to those in uncoordinated dmit (1.68 Å),[38] and 1-methyl-4-imidazoline-2-thione (1.68 Å).[39]

Table 6 Selected bond distances (Å) and angles (°) for **10**

Cu(1)–S(1)	2.3689(10)	S(1)–Cu(1)–S(2)	110.51(5)
Cu(1)–S(2)	2.3748(10)	S(1A)–Cu(1)–S(2)	95.06(4)
Cu(1)–S(3)	2.3347(10)	S(1A)–Cu(1)–S(1)	123.18(2)
Cu(1)–S(1A)	2.3520(10)	S(3)–Cu(1)–S(1)	105.05(4)
Cu(1A)–S(1)	2.3520(10)	S(3)–Cu(1)–S(1A)	105.05(4)
S(1)–C(1)	1.718(3)	S(3)–Cu(1)–S(2)	117.58(3)
S(2)–C(6)	1.698(3)	C(1)–S(1)–Cu(1)	104.53(11)
S(3)–C(14)	1.694(3)	C(6)–S(2)–Cu(1)	99.25(11)

NMR spectroscopy of dinuclear copper thione and selone complexes

The dinuclear copper complexes were characterized by ^1H, $^{13}C\{^1H\}$, $^{77}Se\{^1H\}$, and $^{19}F\{^1H\}$ NMR spectroscopy. In the ^1H NMR spectra of dmit, dmise, Bmm^{Me}, $Bsem^{Me}$, Bme^{Me}, and $Bsee^{Me}$ the olefinic CH protons on the heterocyclic ring are shifted downfield by δ 0.2 to 0.5 from its position in the free ligand upon copper coordination. This same downfield shift was observed by Rabinovich *et al.* for $[Pb_2(Bmm^{Me})_5](ClO_4)_4$,[40] Gardinier *et al.* for $[Ag(mbit)_2]^+$ complexes,[41] and Kimani *et al.* for $[(Tpm^R)Cu(L)]^+$ derivatives (R = H, Me, iPr; L = dmit, dmise).[27] The $^{13}C\{^1H\}$ NMR resonances for the complexed and uncomplexed thione and selone and thione ligands are given in Table 7. Substantial shifting of the *C*=S/*C*=Se resonances of the dmit, dmise, Bmm^{Me}, $Bsem^{Me}$ carbon atoms are observed upon copper complexation relative to the free ligands. Coordination of the thiones and selones *via* the sulfur and selenium atoms results in upfield shifts of δ 5–8 ppm for both the C=S and C=Se carbons, in agreement with previous reports.[34,42]

$^{77}Se\{^1H\}$ NMR spectroscopy studies revealed upfield shifts for the selenium resonances in the copper complexes relative to those of unbound $Bsem^{Me}$ and $Bsee^{Me}$. The $^{77}Se\{^1H\}$ NMR signal for complex **2** could not be obtained, whereas all the complexes with $Bsem^{Me}$ and $Bsee^{Me}$ ligands exhibited upfield selenium resonance shifts of ~40 ppm upon coordination to copper. This upfield shift of the $^{77}Se\{^1H\}$ NMR resonance upon copper binding is direct evidence that the $Bsem^{Me}$ and $Bsee^{Me}$ ligands bind to copper in a bidentate fashion *via* the selenium atoms.

Table 7 $^{13}C\{^1H\}$ and $^{77}Se\{^1H\}$ NMR chemical shifts of the selone and thione ligands

Ligand or complex	*C*=S (dmise)	*C*=Se	^{77}Se
dmit	162.4^t		
dmise		155.6^t	−6
Bmm^{Me}	163.7^b		
$Bsem^{Me}$		157.0^b	16
Bme^{Me}	162.3^b		
$Bsee^{Me}$		155.6^b	22
$[Cu_2(dmit)_5](BF_4)_2$ (**1**)	157.3^t		
$[(dmise)_2Cu(\mu\text{-}dmise)Cu(dmise)_2](BF_4)_2$ (**2**)		147.2	—
$[(Bmm^{Me})Cu(\mu\text{-}Bmm^{Me})Cu(Bmm^{Me})](BF_4)_2$ (**3**)	158.0^b		
$[(Bsem^{Me})Cu(\mu\text{-}Bsem^{Me})Cu(Bsem^{Me})](BF_4)_2$ (**4**)		149.7^b	−28
$[(Bme^{Me})Cu(\mu\text{-}Bme^{Me})Cu(Bme^{Me})](BF_4)_2$ (**5**)	155.2		
$[Cu_2(Bsee^{Me})_3](BF_4)_2$ (**6**)		148.0^b	−43
$[(dmit)Cu(\mu\text{-}Bsem^{Me})_2Cu(dmit)](BF_4)_2$ (**7**)	157.7^t	151.6^b	−24
$[(dmise)Cu(\mu\text{-}Bmm^{Me})_2Cu(dmise)](BF_4)_2$ (**8**)	158.8^b	149.3^t	
$[(dmise)Cu(\mu\text{-}Bsem^{Me})_2Cu(dmise)](BF_4)_2$ (**9**)		149.0^t, 151.3^b	−26
$[(Bmm^{Me})Cu(\mu\text{-}dmit)]_n(BF_4)_n$ (**10**)	156.6^t, 158.4^b		

^{t} = terminal, ^{b} = bridging.

Electrochemical studies of the dinuclear copper complexes

Cyclic voltammetry studies of the chalcogenones and their dinuclear copper complexes were conducted to determine the influence of the methylene linkers on the redox potential of the chalcogenone ligands and the change in Cu(II/I) reduction potential upon coordination of the chalcogenone ligands to copper. All the uncoordinated chalcogenone ligands exhibit chemically reversible and quasi-reversible electrochemical behavior, with the selone ligands having more negative reduction potentials relative to the analogous thione ligands (Fig. 8 and Table 8). The unbound bidentate ethylene-bridged ligands (Bme^{Me} and $Bsee^{Me}$) have larger peak separations between the oxidized and reduced products relative to the methylene-bridged ligands (Bmm^{Me} and $Bsem^{Me}$), suggesting faster electron transfer in the latter.[43]

The reduction potentials of the unbound selone ligands are: dmise −367 mV < $Bsee^{Me}$ (−342 mV) < $Bsem^{Me}$ (−333 mV). The analogous thione ligands follow the same trend: dmit (−169 mV) < Bme^{Me} (−148 mV) < Bmm^{Me} (−118 mV), *versus* normal hydrogen electrode (NHE; Table 8). The reduction potentials of the free bidentate chalcogenones indicate that increasing the length of the linker from methylene to ethylene results in more negative reduction potentials.

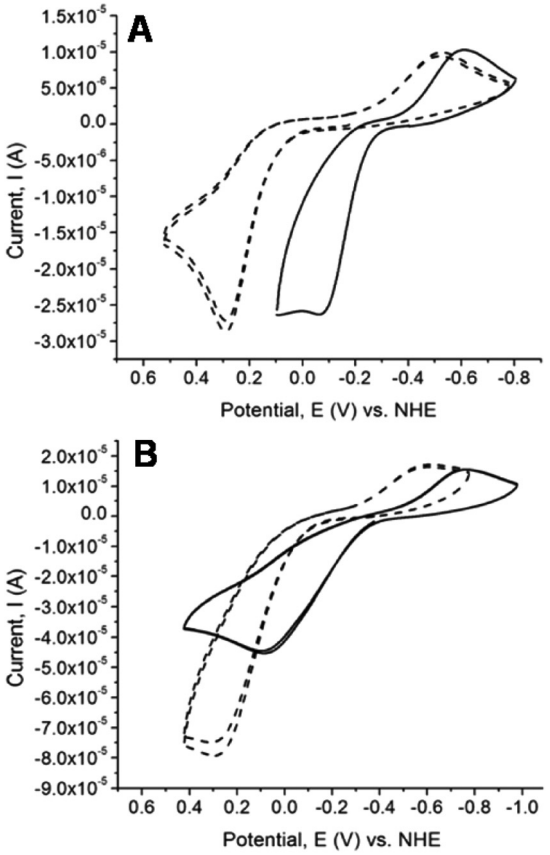

Fig. 8 Cyclic voltammetry (CV) scan for (A) Bmm^{Me} (dashed lines) and $Bsem^{Me}$ (solid lines), (B) Bme^{Me} (dashed lines) and $Bsee^{Me}$ (solid lines). All data were collected with 1 mM complex in acetonitrile.

The Cu(II/I)and Cu(I/0) redox potentials of the complexes *versus* NHE are given in Table 8. The cyclic voltamograms (CV) of the copper complexes **1**, **2**, **3**, **4**, **5**, **6**, **9**, and **10** exhibit two, one-electron redox potential waves belonging to the Cu(II/I)and Cu(I/0) couples, with the exception of complexes **7** and **8** which exhibit three, one-electron redox potential waves. The Cu(I/0) redox couple commences at potentials more than −1000 mV *vs.* NHE and after switching the scan direction at potentials close to 750 mV, Cu(0) is stripped off the electrode (Fig. 9). All the dinuclear copper thione and selone complexes exhibit one-electron Cu(II/I) oxidation and reduction waves with large ΔE values, indicating that these redox processes are not fully reversible (ESI, Fig. S2†).

Upon examination of the reduction potentials for the copper complexes **1**, **2**, **3**, **4**, **5**, and **6**, it is clear that the selone-containing complexes exhibit more negative Cu(II/I) reduction potentials relative to the analogous thione complexes regardless of whether the thione and selone ligands are bridging. A similar trend was reported by Kimani *et al.* for the electrochemistry of only monodentate $[Tpm^{R}Cu(X)]^{+}$ complexes (X = dmise or dmit).[27]

Interestingly, increasing the length of the linker in the bidentate ligands from methylene to ethylene results in lower Cu(II/I) reduction potentials for $[Cu_2(Bsee^{Me})_3](BF_4)_2$ (**6**) (−369 mV) compared to $[Cu_2(Bsem^{Me})_3](BF_4)_2$ (**4**) (−306 mV), and the same trend is observed for the thione complex $[Cu_2(Bme^{Me})_3](BF_4)_2$ (**5**) (−203 mV) relative to $[Cu_2(Bmm^{Me})_3](BF_4)_2$ (**3**) (−180 mV). The dinuclear copper complex **9** with both $Bsem^{Me}$ and dmise ligands has a lower reduction potential of (−356 mV) relative to complex **10** which has both Bmm^{Me} and dmit ligands (−195 mV; Table 8).

The heterogeneous dinuclear complex $[(dmit)_2Cu_2(Bsem^{Me})_2](BF_4)_2$ (**7**) (ESI, Fig. S2I†) exhibits two different reduction and oxidation potentials for the Cu(II/I) couple, whereas $[(dmise)_2Cu_2(Bmm^{Me})_2](BF_4)_2$ (**8**) (ESI, Fig. S2H†) exhibits three oxidation and reduction waves. One reduction and oxidation wave in the dinuclear copper complex **8** likely corresponds to the reduction potential of the bidentate Bmm^{Me} ligand ($E_{1/2}$ = −51 mV), whereas the remaining two waves correspond to Cu(II/I) reduction potentials, similar to those observed for complex **7**. These two different Cu(II/I) reduction potentials are only observed for the dinuclear copper complexes with mixed thione and selone ligands, and effect which has not been previously reported for copper complexes (Table 8).

The unbound dmit and dmise ligands have more negative reduction potentials than the bidentate chalcogenones (Bmm^{Me}, $Bsem^{Me}$, Bme^{Me} and $Bsee^{Me}$). The reduction potentials from the bidentate chalcogenones indicate that increasing the length of the linker from methylene to ethylene results in more negative reduction potentials. All the synthesized copper–selone complexes have more negative Cu(II/I) reduction potentials relative to the analogous copper–thione complexes. The copper–selone complexes stabilize the Cu(II) oxidation state more effectively than the copper–thione complexes by an average of 144 mV, consistent with previously observed results.[27,28]

Table 8 Redox potentials (mV) of chalcogenone ligands and Cu(II/I) and Cu(I/0) couples for dinuclear copper complexes *vs.* NHE all data were collected with 1 mM compound in acetonitrile with *n*-butylammonium phosphate as the supporting electrolyte (0.1 M) at a scan rate of 100 mV s^{-1}

Ligand	E_{pa}	E_{pc}	ΔE	$E_{1/2}$
dmit	424	−761	1158	−167
dmise	39	−773	812	−367
Bmm^{Me}	289	−525	814	−118
$Bsem^{Me}$	−53	−613	560	−333
Bme^{Me}	292	−587	879	−148
$Bsee^{Me}$	83	−768	851	−342

	Cu(II/I)				Cu(I/0)			
Complex	E_{pa}	E_{pc}	ΔE	$E_{1/2}$	E_{pa}	E_{pc}	ΔE	$E_{1/2}$
$[Cu_2(dmit)_5](BF_4)_2$ (**1**)	147	−565	712	−210	−747	−1129	382	−938
$[Cu_2(dmise)_5](BF_4)_2$ (**2**)	−101	−603	502	−352	−724	−1107	383	−920
$[Cu_2(Bmm^{Me})_3](BF_4)_2$ (**3**)	120	−500	620	−180	−742	−1298	556	−1020
$[Cu_2(Bsem^{Me})_3](BF_4)_2$ (**4**)	−37	−575	538	−306	−796	−1336	540	−1066
$[Cu_2(Bme^{Me})_3](BF_4)_2$ (**5**)	228	−634	862	−203	−816	−1299	483	−1058
$[Cu_2(Bsee^{Me})_3](BF_4)_2$ (**6**)	−131	−606	475	−369	−936	−1152	216	−1044
$[(dmit)Cu(\mu\text{-}Bsem^{Me})_2Cu(dmit)](BF_4)_2$ (7)	192, −6	−44, −478	225, 439	74, −242	−710	−1119	409	−915
$[(dmise)Cu(\mu\text{-}Bmm^{Me})_2Cu(dmise)](BF_4)_2$ (**8**)	174, −23	31, −608	149, 585	102, −315	−671	−1107	436	−889
$[(dmise)Cu(\mu\text{-}Bsem^{Me})_2Cu(dmise)](BF_4)_2$ (**9**)	−68	−645	577	−356	−774	−1231	457	−1003
$[(Bmm^{Me})Cu(\mu\text{-}dmit)]_n(BF_4)_n$ (**10**)	147	−535	682	−195	−791	−1222	431	−1007

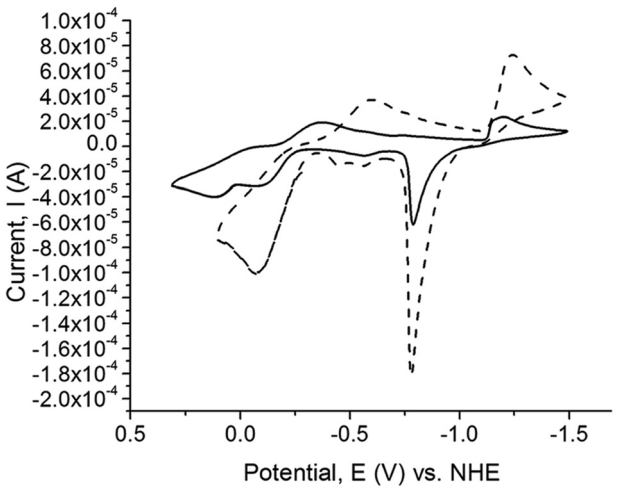

Fig. 9 Cyclic voltammetry (CV) scans for $[(dmit)Cu(\mu\text{-}Bsem^{Me})_2Cu(dmit)](BF_4)_2$ (**7**) (solid line) and $[(dmise)Cu(\mu\text{-}Bsem^{Me})_2Cu(dmise)](BF_4)_2$ (**9**) (dashed line). All data were collected with 1 mM compound in acetonitrile with *n*-butylammonium phosphate as the supporting electrolyte (0.1 M) at a scan rate of 100 mV s^{-1}.

Notably, the Cu(II/I) reduction potential of the dinuclear copper chalcogenone complexes **1** to **10** can be tuned in a 470 mV window from 102 mV to −369 mV by simply changing the nature of the chalcogen donor and the denticity of thione and selone ligands. This ability to tune the copper redox potentials could have potential applications in copper-based catalysis. Compared to naturally occurring cupredoxins with a Cu(II/I) reduction potential range of 90 to 670 mV,[44] the synthesized copper chalcogenone complexes have significantly more negative Cu(II/I) reduction potentials.

Conclusions

Dinuclear homoleptic and heteroleptic copper(I) complexes with monodentate and bidentate chalcogenone ligands have been synthesized and characterized, and the electrochemistry of the resulting species has been investigated and compared. Treating the copper(I) starting material $[Cu(NCMe)_4]BF_4$ with bidentate (Bmm^{Me}, $Bsem^{Me}$, Bme^{Me}, $Bsee^{Me}$) and monodentate chalcogenone ligands (dmit and dmise) results in the formation of dinuclear copper complexes (**1**, **2**, **3**, **4**, **5**, and **6**). The dinuclear copper complexes adopt either trigonal or tetrahedral geometries with both terminal and bridging thione or selone ligands. The heteroleptic dinuclear copper complexes $[(dmit)Cu(\mu\text{-}Bsem^{Me})_2Cu(dmit)](BF_4)_2$ (**7**) and $[(dmise)Cu(\mu\text{-}Bsem^{Me})_2Cu(dmise)](BF_4)_2$ (**9**) adopt distorted tetrahedral geometry where each copper is coordinated to three selenium atoms from $Bsem^{Me}$ ligands and one sulfur atom from dmit for **7** and one selenium atom from dmise for **9**. Interestingly, the mixed ligand complex **10** consists of infinite chains of tetrahedrally coordinated Cu(I) ions bound to two sulfur atoms from a Bmm^{Me} ligand and a bridging sulfur atom from a dmit ligand.

The copper selone complexes **2**, **4**, **6**, and **9** have more negative Cu(II/I) reduction potentials relative to their sulfur analogs (**1**, **3**, **5**, and **10**), and increasing the length of the methylene linker in the bidentate chalcogenone ligands results in more negative reduction potentials for their copper complexes. This study provides detailed comparative coordination chemistry of thiones and selones with copper and its effect on the Cu(II/I) reduction potentials. Simply changing the chalcogens and denticity of the thione and selone ligands results in Cu(II/I) reduction potentials of the synthesized copper chalcogenone complexes that can be tuned in a range of 471 mV, a difference

that would have significant effects in redox-mediated reactions.

Experimental section

Materials

The synthesis and manipulation of all copper complexes was performed under an inert atmosphere of argon or nitrogen using standard Schlenk techniques. Acetonitrile, methanol, and ether were purified using standard procedures and freshly distilled under argon atmosphere prior to use. *N*,*N*′-Dimethylimidazole thione (dmit), *N*,*N*′-dimethylimidazole selone (dmise),[45] $[Cu(NCMe)_4][BF_4]$,[46] bis(mercaptoimidazolyl)methane (Bmm^{Me}), bis(selonoimidazolyl)methane ($Bsem^{Me}$), bis(mercaptoimidazolyl)ethane (Bme^{Me}), and bis(selonoimidazolyl)ethane ($Bsee^{Me}$)[47] were synthesized according to published procedures. The following reagents were used as received: selenium powder (VWR), sulfur powder (VWR), cuprous oxide (stabilized, Aldrich), 1-methylimidazole (VWR), iodomethane (VWR), and dibromomethane (Alfa Aesar).

Instrumentation

^1H, $^{13}C\{^1H\}$, $^{77}Se\{^1H\}$ and $^{19}F\{^1H\}$ spectra were obtained on Bruker-AVANCE 300 and 500 MHz NMR spectrometers. ^1H and $^{13}C\{^1H\}$ NMR chemical shifts (δ) are reported in ppm relative to tetramethylsilane (TMS) and referenced to solvent. $^{19}F\{^1H\}$ NMR spectra were externally referenced to CCl_3F (δ 0 ppm).[48] The $^{77}Se\{^1H\}$ NMR chemical shifts were obtained in $CDCl_3$ and externally referenced to diphenyl diselenide (δ 461 ppm),[49] and reported relative to dimethyl selenide (δ 0 ppm). All ^{77}Se NMR chemical shifts are reported in Table 7.

Electrochemical experiments were performed with a BAS 100B potentiostat. A three-compartment cell was used with an Ag/AgCl reference electrode, Pt counter electrode, and a glassy carbon working electrode. Freshly-distilled acetonitrile was used as the solvent with tetra-*n*-butylammonium phosphate as the supporting electrolyte (0.1 M). Solutions containing 1 mM analyte were deaerated for 2 min by vigorous nitrogen purge. The measured potentials were corrected for junction potentials relative to ferrocenium/ferrocene (0.586 mV *vs.* Ag/AgCl[50]) and adjusted from Ag/AgCl to NHE (−0.197 V (ref. 51)) All $E_{1/2}$ values were calculated from $(E_{pa} + E_{pc})/2$ at a scan rate of 100 mV s^{-1}, and $\Delta E = E_{pa} - E_{pc}$.

Infrared spectra were obtained using Nujol mulls on KBr salt plates with a Magna 550 IR spectrometer. Abbreviations used in the description of vibrational data are as follows: vs, very strong; s, strong; m, medium; w, weak; b, broad. Electrospray ionization mass spectrometry (ESI-MS) was conducted using a QSTAR XL Hybrid MS/MS System from Applied Biosystems *via* direct injection of sample (0.05 mL min^{-1} flow rate) into a Turbo Ionspray ionization source. Samples were run under positive mode, with ionspray voltage of 5500 V, and TOF scan mode. MALDI-TOF-MS was conducted on a Bruker Microflex. *trans*-2-[3-(4-*tert*-Butylphenyl)-2-methyl-2-propenylidene]malononitrile was used as a matrix for co-crystallization of the copper complex characterized. All the peak envelopes matched their calculated isotopic distributions. Melting points were determined using a Barnstead Electrothermal 9100 apparatus in silicon-grease-sealed glass capillary tubes. Absorption spectra were collected using a Varian Cary-50 Bio spectrophotometer in quartz cuvettes with a path length of 1 cm. Elemental analysis (EA) was performed using PerkinElmer Series II CHNS/O Analyzer 2400.

$[Cu_2(dmit)_5](BF_4)_2$ (1)

Dmit (322 mg, 2.5 mmol) was dissolved in acetonitrile (30 mL) and cannula transferred to a solution of $[Cu(NCMe)_4]BF_4$ (312 mg, 1 mmol) in acetonitrile (20 mL). The reaction was stirred at room temperature for 3 h, and the solvent volume was reduced *in vacuo* to about 5 mL. The product was precipitated with diethyl ether (10 mL) to afford an off-white solid that was dried *in vacuo*. Yield: 74% (350 mg, 0.371 mmol). Mp = 132 °C. NMR (CD_3CN): ^1H δ 3.63 (s, 6 H, C*H*$_3$), 6.99 (s, 2 H, C*H*); $^{13}C\{^1H\}$ δ 35.1 (*C*H$_3$), 120.4 (*C*H), 157.3 (*C*═S). IR (cm^{-1}): 521 s, 672 vs, 724 vs, 746 vs, 801 s, 1047 b, 1175 vs, 1236 vs, 1284 v, 1378 s, 1464 vs, 1569 vs, 1684 w, 2276 s, 2304 s, 2723 w, 2859 b, 3118 w, 3142 w. MALDI-TOF-MS: 319.51 $[Cu(dmit)_2]^+$. Anal. Calc. for $C_{25}H_{40}Cu_2N_{10}S_5B_2F_8$: C, 31.89; N, 14.87; H, 4.28. Found: C, 31.80; N, 14.56; H, 4.23%.

$[(dmise)_2Cu(\mu\text{-}dmise)Cu(dmise)_2](BF_4)_2$ (2)

Complex **2** was prepared following the procedure for **1** except dmise (437 mg, 2.5 mmol) was used in place of dmit. Yield: 85% (496 mg, 0.425 mmol). Mp = 126 °C. NMR (CD_3CN): ^1H δ 3.69 (s, 6 H, C*H*$_3$), 7.16 (s, 2 H, C*H*); $^{13}C\{^1H\}$ δ 37.1 (*C*H$_3$), 121.6 (*C*H), 147.2 (*C*═Se); $^{19}F\{^1H\}$ δ −151.62, −151.63. IR (cm^{-1}): 521 s, 624 w, 660 s, 744 s, 933 s, 1021 b, 1238 s, 1285 s, 1378 s, 1457 s, 1570 s, 1818 w, 2252 w, 2276 vs, 2304 vs, 2918 b, 3139 w, 3172 w, 3230 w. MALDI-TOF-MS: 415.07 $[Cu(dmise)_2]^+$. Anal. Calc. for $C_{25}H_{40}Cu_2N_{10}Se_5B_2F_8$: C, 25.53; N, 11.91; H, 3.43. Found: C, 25.42; N, 11.73; H, 3.45%. Single crystals suitable for X-ray analysis were obtained by slow diffusion of diethyl ether into an acetonitrile solution of the complex.

$[(Bmm^{Me})Cu(\mu\text{-}Bmm^{Me})Cu(Bmm^{Me})](BF_4)_2$ (3)

Tetrahydrofuran (5 mL) was added to a 4-dram vial containing a mixture of $[Cu(NCMe)_4]BF_4$ (131 mg, 0.416 mmol) and Bmm^{Me} (150 mg, 0.624 mmol), resulting in the immediate formation of a white solid suspended in a colorless solution. After stirring the suspension for 18 h, the product was isolated by filtration and dried *in vacuo* for 2 h. Yield: 88% (187 mg, 0.183 mmol). Mp = 128 °C. NMR (d_6-DMSO): ^1H δ 3.43 (s, 18 H, C*H*$_3$), 6.59 (s, 6 H, C*H*$_2$), 7.38 (s, 6 H, imidazole *H*), 7.62 (s, 6 H, imidazole *H*); ^{13}C δ 35.9 (q, ^1JC–H = 142, 6 C, *C*H$_3$), 56.3 (t, ^1JC–H = 158, 3 C, *C*H$_2$), 118.8 (dd, ^1JC–H = 201, ^2JC–H = 11, 6 C, imidazole *C*), 121.1 (dd, ^1JC–H = 200, ^2JC–H = 9, 6 C, imidazole *C*), 155.8 (s, 6 C, *C*═S); $^{19}F\{^1H\}$ δ −151.57, −151.63. UV-vis (CH_3CN): 274 nm. IR (cm^{-1}): 3173 m, 3140 m, 3119 m, 3027 w, 2903 w, 2943 m, 1575 s, 1467 vs, 1401 vs, 1378 s, 1317 m, 1286 w, 1249 s, 1215 s, 1166 m, 1064 vs, 788 m, 762 s, 742 s, 724 m, 701 w, 655 w, 521 m, 470 w. Anal. Calc. for

$C_{27}H_{36}B_2Cu_2F_8N_{12}S_6$: C, 31.74; H, 3.55; N, 16.45. Found: C, 31.93; H, 3.56; N, 16.32%. Single crystals suitable for X-ray analysis were obtained by slow diffusion of diethyl ether into an acetonitrile solution of the complex.

[(Bsem^{Me})Cu(μ-Bsem^{Me})Cu(Bsem^{Me})](BF$_4$)$_2$ (4)

Bsem^{Me} (215 mg, 0.75 mmol) was dissolved in dichloromethane (20 mL) before being cannula transferred to a solution of [Cu(NCMe)$_4$]BF$_4$ (160 mg, 0.5 mmol) in acetonitrile (10 mL). The reaction mixture was stirred at room temperature for 3 h. The solvent volume in the reaction mixture was then reduced to about 5 mL and the product was precipitated with diethyl ether. The growth of single crystals for X-ray analysis was performed from slow vapor diffusion of diethyl ether into acetonitrile solution. Yield: 45% (262 mg, 0.225 mmol). Mp = 139 °C. NMR (d$_6$-DMSO): ^{1}H δ 3.54 (s, 6 H, CH_3), 6.82 (s, 2 H, CH_2), 7.33 (d, J_{HH} = 2.0, 2 H, CH), 7.59 (d, J_{HH} = 2.0, 2 H, CH); ^{13}C{^{1}H} δ 37.5 (*C*H$_3$), 59.7 (*C*H$_2$), 121.3 (*C*H), 123.4 (*C*H), 149.7 (*C*=Se); ^{19}F{^{1}H} δ −151.59, −151.63. UV-vis (CH$_3$CN): 292 nm. IR (cm^{-1}): 460 s, 473 w, 521 vs, 604 w, 655 s, 697 s, 731 vs, 779 w, 790 s, 1059 b, 1207 s, 1234 s, 1249 s, 1318 s, 1378 s, 1464 vs, 1575 vs, 1676 vs, 2727 b, 3145 w. Mass spectrum (ESI-MS): *m*/*z* 1216.59 [Cu$_2$(Bsem^{Me})$_3$(BF$_4$)]$^+$, 882.68 [Cu$_2$(Bsem^{Me})$_2$(BF$_4$)]$^+$, 796.67 [Cu$_2$(Bsem^{Me})$_2$]$^{2+}$, 398.83 [Cu(Bsem^{Me})]$^+$. Anal. Calc. for $C_{29}H_{39}Cu_2N_{13}Se_6B_2F_8$: C, 25.91; N, 13.55; H, 2.92. Found: C, 25.98; N, 13.12; H, 3.04%. Single crystals suitable for X-ray analysis were obtained by slow diffusion of diethyl ether into an acetonitrile solution of the complex.

[(Bme^{Me})Cu(μ-Bme^{Me})Cu(Bme^{Me})](BF$_4$)$_2$ (5)

Complex **5** was prepared following the procedure for **4** except Bme^{Me} (191 mg, 0.75 mmol) was used in place of Bsem^{Me}. Yield: 47% (252 mg, 0.236 mmol). Mp = 230 °C. NMR (d$_6$-DMSO): ^{1}H δ 3.52 (s, 6 H, CH_3), 4.63 (s, 4 H, CH_2), 7.18 (d, 2 H, CH), 7.30 (d, 2 H, CH); ^{13}C{^{1}H} δ 35.6 (*C*H$_3$), 45.7 (*C*H$_2$), 119.7 (*C*H), 120.9 (*C*H), 155.2 (*C*=S); ^{19}F{^{1}H} δ −148.31, −148.35. UV-vis (CH$_3$CN): 273 nm. IR (cm^{-1}): 501 w, 522 s, 622 w, 670 s, 680 s, 720 vs, 736 vs, 1059 vs, 1137 w, 1197 s, 1227 s, 1247 vs, 1287 w, 1378 vs, 1415 vs, 1466 vs, 1570 vs, 1694 w, 2927 b, 3137 w. Anal. Calc. for $C_{30}H_{42}Cu_2N_{12}S_6B_2F_8$: C, 33.87; N, 15.50; H, 3.98. Found: C, 29.88; N, 13.68; H, 3.45%.

[Cu$_2$(Bsee^{Me})$_3$](BF$_4$)$_2$ (6)

Complex **6** was prepared following the procedure for **4** except that Bsee^{Me} (223 mg, 0.75 mmol) was used in place of Bsem^{Me}. Yield: 30% (174 mg, 0.153 mmol). Mp = 270 °C. NMR (d$_6$-DMSO): ^{1}H δ 3.58 (s, 6 H, CH_3), 4.73 (s, 4 H, CH_2), 7.33 (d, 2 H, CH), 7.47 (d, 2 H, CH); ^{13}C{^{1}H} δ 39.7 (*C*H$_3$), 47.5 (*C*H$_2$), 121.5 (*C*H), 122.8 (*C*H), 148.0 (*C*=Se); ^{19}F{^{1}H} δ −148.10, −148.16. UV-vis (CH$_3$CN): 288 nm. IR (cm^{-1}): 522 s, 666 vs, 724 vs, 738 vs, 747 vs, 800 w, 930 w, 1057 vs, 1128 vs, 1183 vs, 1223 s, 1246 vs, 1287 w, 1378 vs, 1409 vs, 1467 vs, 1569 vs, 2854 vs, 2919 b, 3114 w, 3146 w, 3173 w. Anal. Calc. for $C_{30}H_{42}Cu_2N_{12}Se_6B_2F_8$: C, 26.79; N, 12.49; H, 3.15. Found: C, 26.97; N, 12.48; H, 3.12%.

[(dmit)Cu(μ-Bsem^{Me})$_2$Cu(dmit)](BF$_4$)$_2$ (7)

Dmit (129 mg, 1 mmol) was dissolved in acetonitrile (20 mL) and cannula transferred to a solution of [Cu(NCMe)$_4$]BF$_4$ (312 mg, 1 mmol) in acetonitrile (10 mL). The reaction was stirred at room temperature for 3 h, resulting in the formation of a yellow solution. To this reaction mixture was cannula added Bsem^{Me} (336 mg, 1 mmol) in dichloromethane (10 mL) and stirred overnight. The solvent volume was reduced *in vacuo* to about 3 mL and the product was precipitated with diethyl ether to afford an off-white solid, which was dried *in vacuo*. Yield: 38% (427 mg, 0.378 mmol). Mp = 209 °C. NMR (CD$_3$CN): ^{1}H δ 3.60 (s, 6 H, CH_3), 3.62 (s, 6 H, CH_3), 6.65 (s, 2 H, CH_2), 6.98 (s, 2 H, CH), 7.23 (d, J_{HH} = 2.5, 2 H, CH), 7.38 (d, J_{HH} = 2.0, 2 H, CH); ^{13}C{^{1}H} δ 35.8 (*C*H$_3$), 37.8 (*C*H$_3$), 60.5 (*C*H$_2$), 120.0 (*C*H), 121.0 (*C*H), 123.3 (*C*H), 151.6 [*C*=Se (Bsem^{Me})], 157.7 [*C*=S (dmit)]; ^{19}F{^{1}H} δ −151.52, −151.57. UV-vis (CH$_3$CN): 274 nm. IR (cm^{-1}): 508 s, 521 s, 611 s, 640 s, 650 s, 657 s, 676 s, 723 vs, 746 vs, 790 vs, 839 s, 867 s, 1033 b, 1145 s, 1177 s, 1207 s, 1229 s, 1249 s, 1290 s, 1321 s, 1372 s, 1395 s, 1465 s, 1571 vs, 1602 s, 1673 s, 2920 b, 3088 s. Mass spectrum (ESI-MS): *m*/*z* 732.73 [Cu(Bsem^{Me})$_2$]$^+$, 526.85 [(dmit)-Cu(Bsem^{Me})]$^+$, 398.82 [Cu(Bsem^{Me})]$^+$, 318.97 [Cu(dmit)$_2$]$^+$, 190.95 [Cu(dmit)]$^+$. Anal. Calc. for $C_{28}H_{40}Cu_2N_{12}Se_4S_2B_2F_8$: C, 27.44; N, 13.72; H, 3.29. Found: C, 27.28; N, 13.60; H, 3.27%. Single crystals suitable for X-ray analysis were obtained by slow diffusion of diethyl ether into an acetonitrile solution of the complex.

[(dmise)Cu(μ-Bmm^{Me})$_2$Cu(dmise)](BF$_4$)$_2$ (8)

Complex **8** was prepared following the same procedure for **7** except that dmise (176 mg, 1 mmol) was used in place of dmit and Bmm^{Me} (242 mg, 1 mmol) was used in place of Bsem^{Me}. Yield: 30% (347 mg, 0.302 mmol). Mp = 174 °C. NMR (CD$_3$CN): ^{1}H δ 3.52 (s, 6 H, CH_3, Bmm^{Me}), 3.69 (s, 6 H, CH_3, dmise), 6.48 (s, 2 H, CH$_2$), 7.04 (d, J_{HH} = 3.0, 2 H, CH), 7.14 (s, 2 H, CH, dmise), 7.26 (d, J_{HH} = 3.0, 2 H, CH); ^{13}C{^{1}H} δ 35.9 (*C*H$_3$), 37.7 (*C*H$_3$), 57.5 (*C*H$_2$), 118.9 (*C*H), 121.4 (*C*H), 122.5 (*C*H), 149.3 [*C*=Se (dmise)], 158.8 [C=S (Bmm^{Me})]; ^{19}F{^{1}H} δ −151.48, −151.53. UV-vis (CH$_3$CN): 269 nm. IR (cm^{-1}): 521 s, 672 vs, 725 vs, 741 vs, 761 vs, 796 vs, 848 s, 983 s, 1033 b, 1217 vs, 1234 vs, 1250 vs, 1287 s, 1314 s, 1376 vs, 1401 vs, 1429 s, 1464 b, 1571 vs, 1699 b, 2851 b, 3141 s, 3171 s. Anal. Calc. for $C_{28}H_{40}Cu_2N_{12}Se_2S_4B_2F_8$: C, 29.72; N, 14.85; H, 3.56. Found: C, 29.60; N, 14.61; H, 3.53%. Single crystals suitable for X-ray analysis were obtained by slow diffusion of diethyl ether into an acetonitrile solution of the complex.

[(dmise)Cu(μ-Bsem^{Me})$_2$Cu(dmise)](BF$_4$)$_2$ (9)

Complex **9** was prepared following the same procedure for **7** except that dmise (176 mg, 1 mmol) was used instead of dmit. Yield: 46% (558 mg, 0.456 mmol). Mp = 193 °C. NMR (CD$_3$CN): ^{1}H δ 3.62 (s, 6 H, CH_3), 3.68 (s, 6 H, CH_3), 6.68 (s, 2 H, CH_2), 7.14 (s, 2 H, CH), 7.24 (d, J_{HH} = 2.0, 2 H, CH), 7.40 (d, J_{HH} = 2.0, 2 H, CH); ^{13}C{^{1}H} δ 36.5 (*C*H$_3$), 37.8 (*C*H$_3$), 60.5 (*C*H$_2$), 121.1 (*C*H), 122.0 (C*H*), 123.7 (*C*H), 149.0 [*C*=Se

(dmise)], 151.3 [*C*═Se (Bsem^{Me})]; $^{19}F\{^1H\}$ δ −151.56, −151.61. UV-vis (CH_3CN): 278 nm. IR (cm^{-1}): 521 s, 623 s, 650 s, 658 s, 724 s, 745 s, 791 s, 837 s, 1055 b, 1176 s, 1207 s, 1230 vs, 1248 s, 1287 s, 1320 s, 1378 b, 1464 vs, 1571 vs, 1673 s, 2925 b, 3132 b. Mass spectrum (ESI-MS): *m*/*z* 732.76 $[Cu(Bsem^{Me})_2]^+$, 572.81 $[(dmise)Cu(Bsem^{Me})]^+$, 398.83 $[Cu(Bsem^{Me})]^+$, 239.02 $[Cu(dmise)]^+$. Anal. Calc. for $C_{28}H_{40}Cu_2N_{12}Se_6B_2F_8$: C, 25.49; N, 12.74; H, 3.06. Found: C, 24.85; N, 12.48; H, 3.00%. Single crystals suitable for X-ray analysis were obtained by slow diffusion of diethyl ether into an acetonitrile solution of the complex.

$[(Bmm^{Me})Cu(\mu\text{-dmit})]_n(BF_4)_n$ (10)

Complex **10** was prepared following the same procedure for **7** except that Bmm^{Me} (242 mg, 1 mmol) was used instead of Bsem^{Me}. Yield: 34% (354 mg, 0.335 mmol). Mp = 159 °C. NMR (CD_3CN): ^1H δ 3.52 (s, 6 H, CH_3, Bmm^{Me}), 3.62 (s, 6 H, CH_3, dmit), 6.49 (s, 2 H, CH_2), 7.00 (s, 2 H, C*H*), 7.06 (d, J_{HH} = 2.5, 2 H, C*H*), 7.25 (d, J_{HH} = 2.5, 2 H, C*H*); $^{13}C\{^1H\}$ δ 35.9 (*C*H_3), 57.5 (*C*H_2), 119.0 (*C*H), 120.3 (*C*H), 121.5 (*C*H), 156.6 [*C*═S (dmit)], 158.4 [*C*═S (Bmm^{Me})]; $^{19}F\{^1H\}$ δ −151.30, −151.35. UV-vis (CH_3CN): 268 nm. IR (cm^{-1}): 503 s, 521 s, 603 s, 633 s, 670 vs, 729 vs, 760 s, 782 s, 848 s, 1032 b, 1174 s, 1234 vs, 1286 s, 1395 vs, 1464 vs, 1572 vs, 1684 b, 2250 s, 2725 s, 2921 b, 3140 b. Anal. Calc. for $C_{28}H_{40}Cu_2N_{12}S_6B_2F_8$: C, 32.41; N, 16.20; H, 3.88. Found: C, 32.55; N, 16.15; H, 3.97%. Single crystals suitable for X-ray analysis were obtained by slow diffusion of diethyl ether into an acetonitrile solution of the complex.

X-ray data collection and structural determination

Single crystals grown from vapor diffusion were mounted on a glass filament with silicon grease and immediately cooled to 168 K in a cold nitrogen gas stream. Single crystals suitable for X-ray analysis were obtained by slow diffusion of diethyl ether into an acetonitrile solution of $[(dmise)_2Cu(\mu\text{-dmise})Cu(dmise)_2](BF_4)_2$ (**2**), $[(Bmm^{Me})Cu(\mu\text{-}Bmm^{Me})Cu(Bmm^{Me})](BF_4)_2$ (**3**), $[(Bsem^{Me})Cu(\mu\text{-}Bsem^{Me})Cu(Bsem^{Me})](BF_4)_2$ (**4**), $[(Bme^{Me})Cu(\mu\text{-}Bme^{Me})Cu(Bme^{Me})](BF_4)_2$ (**5**), $[(dmit)Cu(\mu\text{-}Bsem^{Me})_2Cu(dmit)](BF_4)_2$ (**7**), $[(dmise)Cu(\mu\text{-}Bsem^{Me})_2Cu(dmise)](BF_4)_2$ (**9**), and $[(Bmm^{Me})Cu(\mu\text{-dmit})]_n(BF_4)_n$ (**10**). Intensity data were collected using a Rigaku Mercury CCD detector and an AFC8S diffractometer. The space group $P2_1/c$ for **9** was determined from the observed systematic absences. No symmetry higher than triclinic was observed for **2**, **4**, **5**, **7**, and **10** and assignment of the centrosymmetric space group option, $P\bar{1}$, provided chemically reasonable refinement results. Data reduction including the application of Lorentz and polarization (Lp) effects and absorption corrections used the CrystalClear program.[52] The structures were solved by direct methods and subsequent Fourier difference techniques, and refined anisotropically, by full-matrix least squares, on F^2 using SHELXTL 6.10.[53] In the final cycle of least squares, independent anisotropic displacement factors were refined for the non-hydrogen atoms and the methyl hydrogen atoms were fixed in "idealized" positions with C–H = 0.96 Å. Their isotropic displacement parameters were set equal to 1.5 times U_{eq} of the attached carbon atom.

Table 9 Summary of crystallographic data for complexes **2**, **3**, **4**, and **5**

	2	**4**	**3**	**5**
Chemical formula	$C_{27}H_{43}B_2Cu_2F_8N_{11}Se_5$	$C_{29}H_{39}B_2Cu_2F_8N_{13}Se_6$	$C_{27}H_{36}B_2Cu_2F_8N_{12}Se_6$	$C_{33}H_{46}Cu_2N_{13}S_6B_2F_8$
F.W. (g mol^{-1})	1217.22	1344.19	1021.74	1437.29
Space group	$P\bar{1}$	$P\bar{1}$	*Pna*2(1)	$P\bar{1}$
Crystal system	Triclinic	Triclinic	Orthorhombic	Triclinic
a, Å	11.712(2)	11.972(2)	14.997(7)	10.368(2)
b, Å	14.126(3)	14.325(3)	15.362(7)	10.699(2)
c, Å	14.800(3)	15.568(3)	17.487(8)	10.804(2)
α, °	87.32(3)	89.58(3)	90	98.29(3)
β, °	73.78(3)	77.29(3)	90	116.81(3)
γ, °	71.01(3)	68.69(3)	90	91.25(3)
V, Å^3	2220.5(8)	2418.7(8)	4029(3)	1053.4(4)
Z	2	2	4	2
D_{cal}, mg m^{-3}	1.821	1.846	1.685	1.677
Indices (min)	[−14, −17, −18]	[−14, −17, 0]	[−19, −20, −23]	[−12, −11, −13]
(max)	[14, 17, 18]	[14, 17, 19]	[19, 19, 22]	[12, 11, 13]
Parameters	508	548	520	274
F(000)	1184	1296	2072	542
μ, mm^{-1}	5.124	5.462	1.444	1.384
2θ range, °	3.19–26.38	2.94–26.34	1.76–28.24	3.09–26.30
Collected reflections	18 943	9716	40 237	9129
Unique reflections	8943	9716	9227	9129
Final *R* (obs. data)[a], R_1	0.0461	0.0470	0.0527	0.0553
wR_2	0.1125	0.1116	0.1267	0.1363
Final *R* (all data), R_1	0.0616	0.0666	0.0682	0.0553
wR_2	0.1263	0.1276	0.1371	0.1581
Goodness of fit (*S*)	1.117	1.062	1.006	1.046
Largest diff. peak	1.081	0.817	1.107	0.929
Largest diff. hole	−0.813	−0.792	−1.468	−0.880

[a] $R_1 = [\sum||F_o| - |F_c||]/\sum|F_o|$; $wR_2 = \{[\sum w[(F_o)^2 - (F_c)^2]^2\}^{1/2}$.

Table 10 Summary of crystallographic data for complexes **7**, **9**, and **10**

	9	**7**	**10**
Chemical formula	$C_{28}H_{40}Cu_2N_{12}Se_6B_2F_8$	$C_{28}H_{40}Cu_2N_{12}S_2Se_4B_2F_8$	$C_{28}H_{40}Cu_2N_{12}S_6B_2F_8$
F.W. (g mol^{-1})	1319.18	1225.38	1037.78
Space group	$P\bar{1}$	$P\bar{1}$	$P2_1/c$
Crystal system	Triclinic	Triclinic	Monoclinic
a, Å	8.21868(16)	8.1987(16)	9.4763(19)
b, Å	11.247(2)	11.198(2)	27.970(6)
c, Å	12.904(3)	12.935(3)	7. 8016(16)
α, °	66.67(3)	65.68(3)	90
β, °	84.64(3)	84.17(3)	99. 89 (3)
γ, °	77.72(3)	77.75(3)	90
V, Å^3	1066.1(4)	1057.5(4)	2037.1(7)
Z	1	1	2
D_{cal}, Mg m^{-3}	2.055	1.924	1.692
Indices (min)	[−10, −14, 16]	[−12, −21, −24]	[−11, −34, −7]
(max)	[9, 14, 11]	[11, 21, 26]	[11, 34, 9]
Parameters	266	267	266
F(000)	636	600	1056
μ, mm^{-1}	6.194	4.622	1.429
2θ range, °	3.12–26.75	2.95–26.35	2.18–26.31
Collected reflections	9066	8161	16 881
Unique reflections	4435	4221	4096
Final R (obs. data)[a], R_1	0.0503	0.0455	0.0440
wR_2	0.1120	0.1049	0.0984
Final R (all data), R_1	0.0796	0.0658	0.0591
wR_2	0.1319	0.1182	0.1074
Goodness of fit (S)	1.093	1.100	1.089
Largest diff. peak	1.158	1.097	0.416
Largest diff. hole	−0.736	−0.778	−0.424

[a] $R_1 = [\sum||F_o| - |F_c||]/\sum|F_o|$; $wR_2 = \{[\sum w[(F_o)^2 - (F_c)^2]^2]\}^{1/2}$.

For complex **2**, the largest peak in the final Fourier difference map (1.08 e A^{-3}) was located 0.83 Å from Se(4) and the lowest peak (−0.81 e A^{-3}) was located at a distance of 0.86 Å from Se(4). The largest peak for complex **4** in the final Fourier difference map (0.82 e A^{-3}) was located 0.08 Å from Se(4) and the lowest peak (−0.79 e A^{-3}) was located at a distance of 0.77 Å from Se(5). The largest peak for **7** in the final Fourier difference map (1.10 e A^{-3}) was located 1.23 Å from N(5) and the lowest peak (−0.78 e A^{-3}) was located at a distance of 0.88 Å from Se(1). The largest peak for **9** in the final Fourier difference map (1.16 e A^{-3}) was located 1.19 Å from H(6C) and the lowest peak (−0.74 e A^{-3}) was located at a distance of 0.92 Å from Se(1). The largest peak for **10** in the final Fourier difference map (0.42 e A^{-3}) was located 1.73 Å from S(1), and the lowest peak (−0.42 e A^{-3}) was located at a distance of 0.76 Å from Cu(1).

For complex **3**, a suitable crystal was mounted using viscous oil onto a plastic mesh, and cooled to the data collection temperature. Data were collected on a Bruker-AXS APEX CCD diffractometer with graphite-monochromated Mo-Kα radiation (λ = 0.71073 Å). The systematic absences in the diffraction data were consistent with $Pna2_1$ and $Pnma$. The absence of a molecular mirror or inversion point, and the observed occupancy, Z = 4, were consistent with $Pna2_1$, the noncentrosymmetric option. The Flack parameter refined to zero, indicating that the true hand of the data was determined. This data set was treated with absorption corrections based on redundant multiscan data. The structures were solved using direct methods and refined with full-matrix, least-squares procedures on F^2. All non-hydrogen atoms were refined with anisotropic displacement parameters. All hydrogen atoms were treated as idealized contributions. Scattering factors are contained in the SHELXTL 6.12 program library.[54] Final refinement parameters for the structures of **2**, **3**, **4**, **5**, **7**, **9**, and **10** are provided in Tables 9 and 10.

Acknowledgements

J.L.B. thanks the National Science Foundation for a CAREER Award (CHE-0545138) and additional financial support from grant CHE-1213912. D.R. also acknowledges financial support from the National Science Foundation (CHE-0911407) and The University of North Carolina at Charlotte. M.M.K. thanks the Clemson University Chemistry Department for a graduate fellowship. We thank Carolyn E. Quarles for performing the ESI-MS experiments.

References

1 W.-G. Jia, Y.-B. Huang, Y.-J. Lin and G.-X. Jin, *Dalton Trans.*, 2008, 5612–5620.
2 H. R. Kim, I. G. Jung, K. Yoo, K. Jang, E. S. Lee, J. Yun and S. U. Son, *Chem. Commun.*, 2010, **46**, 758–760.
3 L. Maria, C. Moura, A. Paulo, I. C. Santos and I. Santos, *J. Organomet. Chem.*, 2006, **691**, 4773–4778.

4 G. Parkin, *New J. Chem.*, 2007, **31**, 1996–2014.
5 G. Roy, P. N. Jayaram and G. Mugesh, *Chem. – Asian J.*, 2013, **8**, 1910–1921.
6 C. Kimblin, B. M. Bridgewater, D. G. Churchill, T. Hascall and G. Parkin, *Inorg. Chem.*, 2000, **39**, 4240–4243.
7 C. Kimblin, T. Hascall and G. Parkin, *Inorg. Chem.*, 1997, **36**, 5680–5681.
8 D. J. Williams, D. VanDerveer, R. L. Jones and D. S. Menaldino, *Inorg. Chim. Acta*, 1989, **165**, 173–178.
9 V. K. Landry, D. Bucella, K. Pang and G. Parkin, *Dalton Trans.*, 2007, 866–870.
10 V. K. Landry and G. Parkin, *Polyhedron*, 2007, **26**, 4751–4757.
11 W.-G. Jia, Y.-B. Huang, Y.-J. Lin, G.-L. Wang and G.-X. Jin, *Eur. J. Inorg. Chem.*, 2008, 4063–4073.
12 M. O. Awaleh, A. Badia and F. Brisse, *Inorg. Chem.*, 2007, **46**, 3185–3191.
13 N. Kuhn and T. Kratz, *Synthesis*, 1993, 561–562.
14 J. Cheon, J. Arnold, K. M. Yu and E. D. Bourret, *Chem. Mater.*, 1995, **7**, 2273–2276.
15 S. Meyer, S. Demeshko, S. Dechert and F. Meyer, *Inorg. Chim. Acta*, 2010, **363**, 3088–3092.
16 I. R. Crossley, A. F. Hill, E. R. Humphrey and M. K. Smith, *Organometallics*, 2006, **25**, 2242–2247.
17 W.-G. Jia, Y.-B. Huang and G.-X. Jin, *J. Organomet. Chem.*, 2009, **694**, 3376–3380.
18 R. M. Silva, M. D. Smith and J. R. Gardinier, *Inorg. Chem.*, 2006, **45**, 2132–2142.
19 M. T. Aroz, M. C. Gimeno, M. Kulcsar, A. Laguna and V. Lippolis, *Eur. J. Inorg. Chem.*, 2011, 2884–2894.
20 J. Nunn, I. Zahedi, G. Bauer, M. F. Haddow, S. N. A. Halim, A. Pérez-Redondo and G. R. Owen, *Inorg. Chim. Acta*, 2011, **365**, 462–468.
21 F. Bigoli, P. Deplano, F. A. Devillanova, V. Lippolis, M. L. Mercuri, M. A. Pellinghelli and E. F. Trogu, *Inorg. Chim. Acta*, 1998, **267**, 115–121.
22 T. A. Pinder, D. VanDerveer and D. Rabinovich, *Inorg. Chem. Commun.*, 2007, **10**, 1381–1384.
23 D. J. Williams, A. Shilatifard, D. VanDeveer, L. A. Lipscomb and R. L. Jones, *Inorg. Chim. Acta*, 1992, **202**, 53–57.
24 J. Choudhury, P. Sinha, S. Prabhakar, M. Vairamani and S. Roy, *Phosphorus, Sulfur Silicon Relat. Elem.*, 2008, **183**, 2943–2955.
25 N. M. Marshall, D. K. Garner, T. D. Wilson, Y. G. Gao, H. Robinson, M. J. Nilges and Y. Lu, *Nature*, 2009, **462**, 113–117.
26 E. R. Strieter, B. Bhayana and S. L. Buchwald, *J. Am. Chem. Soc.*, 2009, **131**, 78–88.
27 M. M. Kimani, J. L. Brumaghim and D. VanDerveer, *Inorg. Chem.*, 2010, **49**, 9200–9211.
28 M. M. Kimani, J. L. Brumaghim and C. A. Bayse, *Dalton Trans.*, 2011, **40**, 3711–3723.
29 R. Balamurugan, M. Palaniandavar and R. S. Gopalan, *Inorg. Chem.*, 2001, **40**, 2246–2255.
30 D. G. Booth, W. Levason, J. J. Quirk, G. Reid and S. M. Smith, *J. Chem. Soc., Dalton Trans.*, 1997, 3493–3500.
31 A. J. Blake, V. Lippolis, T. Pivetta and G. Verani, *Acta Crystallogr., Sect. C: Cryst. Struct. Commun.*, 2007, **63**, m364–m367.
32 D. J. Williams, M. R. Fawcettbrown, R. R. Raye, D. Vanderveer, Y. T. Pang, R. L. Jones and K. L. Bergbauer, *Heteroat. Chem.*, 1993, **4**, 409–414.
33 F. A. Devillanova, G. Verani, L. P. Battaglia and B. A. Corradi, *Transition Met. Chem.*, 1980, **5**, 362–364.
34 A. Beheshti, W. Clegg, V. Nobakht, M. P. Mehr and L. Russo, *Dalton Trans.*, 2008, 6641–6646.
35 P. Aslanidis, S. K. Hadjikakou, P. Karagiannidis and P. J. Cox, *Inorg. Chim. Acta*, 1998, **271**, 243–247.
36 T. S. Lobana, R. Sharma and R. J. Butcher, *Z. Anorg. Allg. Chem.*, 2008, **634**, 1785–1790.
37 L. Basumallick, S. D. George, D. W. Randall, B. Hedman, K. O. Hodgson, K. Fujisawa and E. I. Solomon, *Inorg. Chim. Acta*, 2002, **337**, 357–365.
38 D. W. Tomlin, D. P. Campbell, P. A. Fleitz and W. W. Adams, *Acta Crystallogr., Sect. C: Cryst. Struct. Commun.*, 1997, **53**, 1153–1154.
39 E. S. Raper, J. R. Creighton, R. E. Oughtred and I. W. Nowell, *Acta Crystallogr., Sect. B: Struct. Commun.*, 1983, **39**, 355–360.
40 T. A. Pinder, D. VanDerveer and D. Rabinovich, *Inorg. Chem. Commun.*, 2007, **10**, 1381–1384.
41 R. M. Silva, M. D. Smith and J. R. Gardinier, *Inorg. Chem.*, 2006, **45**, 2132–2142.
42 T. S. Lobana and A. Castineiras, *Polyhedron*, 2002, **21**, 1603–1611.
43 D. H. Lee, L. Y. Q. Hatcher, M. A. Vance, R. Sarangi, A. E. Milligan, A. A. N. Sarjeant, C. D. Incarvito, A. L. Rheingold, K. O. Hodgson, B. Hedman, E. I. Solomon and K. D. Karlin, *Inorg. Chem.*, 2007, **46**, 6056–6068.
44 C. Dennison, *Coord. Chem. Rev.*, 2005, **249**, 3025–3054.
45 G. Roy, D. Das and G. Mugesh, *Inorg. Chim. Acta*, 2007, **360**, 303–316.
46 G. J. Kubas, *Inorg. Synth.*, 1990, **28**, 68–70.
47 W. G. Jia, Y. B. Huang, Y. J. Lin and G. X. Jin, *Dalton Trans.*, 2008, 5612–5620.
48 R. K. Harris and B. E. Mann, *NMR and the Periodic Table*, Academic Press, London, 1978, p. 99.
49 J. D. Odom, W. H. Dawson and P. D. Ellis, *J. Am. Chem. Soc.*, 1979, **101**, 5815–5823.
50 N. G. Connelly and W. E. Geiger, *Chem. Rev.*, 1996, **96**, 877–910.
51 H. M. Koepp, H. Wendt and H. Z. Strehlow, *Electrochemistry*, 1960, **64**, 483–491.
52 T. H. Dunning, *J. Chem. Phys.*, 1971, **55**, 716–723.
53 G. M. Sheldrick, Bruker Analytical X-ray Systems Inc., Madison, WI, 2000.
54 G. M. Sheldrick, *Acta Crystallogr., Sect. A: Fundam. Crystallogr.*, 2008, **64**, 112–122.